JOURNAL OF NATURAL PRODUCTS

Article

pubs.acs.org/jnp

Tyrosyl-DNA Phosphodiesterase 1 Inhibitors: Usnic Acid Enamines Enhance the Cytotoxic Effect of Camptothecin

Alexandra Zakharenko,[†,#] Olga Luzina,[‡,#] Olga Koval,[†,§] Dmitry Nilov,[⊥] Irina Gushchina,[∥] Nadezhda Dyrkheeva,[†] Vytas Švedas,[⊥,∥] Nariman Salakhutdinov,[‡,§] and Olga Lavrik*[,†,§]

[†]Novosibirsk Institute of Chemical Biology and Fundamental Medicine, Siberian Branch of the Russian Academy of Sciences, Novosibirsk, 630090, Russian Federation

[‡]N. N. Vorozhtsov Novosibirsk Institute of Organic Chemistry, Siberian Branch of the Russian Academy of Sciences, Novosibirsk, 630090, Russian Federation

[§]Novosibirsk State University, Novosibirsk, 630090, Russian Federation

[⊥]Belozersky Institute of Physicochemical Biology and [∥]Faculty of Bioengineering and Bioinformatics, Lomonosov Moscow State University, Moscow, 119991, Russian Federation

Supporting Information

ABSTRACT: Tyrosyl-DNA phosphodiesterase 1 (TDP1) is a repair enzyme for stalled DNA-topoisomerase 1 (Top1) cleavage complexes and other 3′-end DNA lesions. TDP1 is a perspective target for anticancer therapy based on Top1-poison-mediated DNA damage. Several novel usnic acid derivatives with an enamine moiety have been synthesized and tested as inhibitors of TDP1. The enamines of usnic acid showed IC_{50} values in the range of 0.16 to 2.0 μM. These compounds revealed moderate cytotoxicity against human tumor MCF-7 cells. These new compounds enhanced the cytotoxicity of the established Top1 poison camptothecin by an order of magnitude.

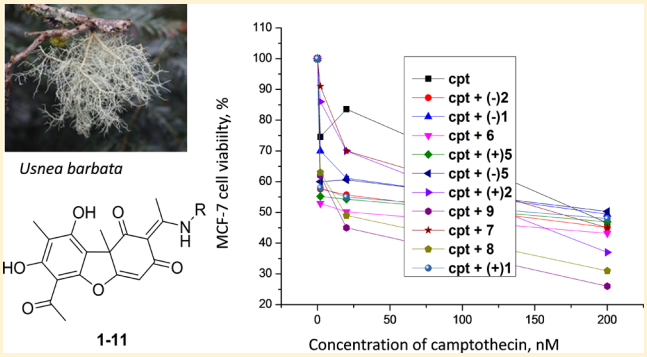

Usnic acid (UA) is the best known lichen secondary metabolite. It is produced by *Cladonia* (Cladoniaceae), *Usnea* (Usneaceae), *Lecanora* (Lecanoraceae), *Ramalina* (Ramalinaceae), *Evernia*, *Parmelia* (Parmeliaceae), *Alectoria* (Alectoriaceae), and other lichen genera.[1] UA has been of interest to chemists and pharmacologists owing to the broad range of its biological activity, such as antitumor, antiviral, antimicrobial, anti-inflammatory, and insecticidal effects.[1] It is one of the few commercially available lichen metabolites and has been the most extensively investigated. In the 1990s, it was reported that UA has hepatotoxicity observed following long-term consumption of large UA doses.[2] However, in spite of the limitations imposed by UA toxicity, its biological properties continue to be studied, and up-to-date research methods provide intimate knowledge of biological mechanisms that mediate its action as well as expand the scope of practical applications.

In recent decades, structure−activity studies designed to reduce the side effects of UA have been conducted. These efforts have ultimately led to the discovery of lead compounds with better pharmacological and toxicity profiles.[3,4] The synthesis of new UA derivatives[5] and the investigation of their biological activity contributes much to the understanding of the biological action of UA itself and opens up fresh opportunities for the pharmacological use of this metabolite. The currently known structure-to-property relationships suggest that the UA enamine derivatives have some improved biological properties in comparison with a native UA. Such UA derivatives as enamines isolated from *Usnea longissima* inhibit the growth of human hepatoma HepG2 cells and reveal high antifungal and antibacterial activities.[6]

The main mechanism underlying the moderate cytotoxic activity of UA is apoptosis via the intrinsic pathway.[4] It is known that UA has specific effects on tumors, which include suppression of cell colony growth as well as inhibition of angiogenesis.[4] The decreased cytotoxicities of the UA enamine derivatives recently reported by Bazin et al. indicate high antitumor potential of the synthetic agents.[7]

The development of inhibitors of DNA repair pathways is one of the main goals of medicinal chemistry. The elaboration of drugs based on inhibition of DNA repair systems can provide a new effective treatment for cardiovascular, oncological, and neurodegenerative diseases. These pathologies are often associated with DNA repair abnormalities.[8−10]

Tyrosyl-DNA phosphodiesterase I (TDP1) is associated with the human neurodegenerative disease SCAN1[11] (spinocerebellar ataxia with axonal neuropathy) and protects cancer cells

Received: October 25, 2016

DOI: 10.1021/acs.jnatprod.6b00979
J. Nat. Prod. XXXX, XXX, XXX−XXX

from certain types of chemotherapy.[12] TDP1 is implicated in the processing of different 3′-lesions,[13] including stalled Top1−DNA covalent complexes (Top1cc) processed by proteasomal degradation,[14] and Top1cc are stabilized by Top1 inhibitors, such as camptothecin and some other anticancer drugs (for review see ref 11). The inability to reseal Top1cc leads to the formation of DNA single-strand breaks that can be turned into more toxic double-strand breaks, thus resulting in cell death or chromosomal translocations. Inhibiting the activity of TDP1 one can enhance the therapeutic effect of clinical Top1 inhibitors.[15,16] This is confirmed by several studies: tdp1−/− mice and human cell lines with SCAN1 mutation are hypersensitive to camptothecin.[13,17] Furthermore, camptothecin causes less DNA damages in cells with high TDP1 expression.[18−21] A positive correlation has been observed between the percentage of NSCLC (non-small-cell lung cancer) cells in tumor tissues and TDP1 activity.[22]

A few TDP1 inhibitors have been described in the literature, and they all demonstrate moderate activity with IC_{50} values (concentration of a compound required to reduce the enzyme activity by 50%) in the concentration range of 0.4 to 100 μM.[13,23−30] Two classes of TDP1 inhibitors have also been reported by our group: diazaadamantane derivatives (IC_{50} values from 15 to 68 μM)[31] and more effective benzopentathiepine derivatives (IC_{50} values from 0.2 to 6 μM).[32] In this paper we present efficient inhibitors of TDP1 with a novel structural motif. Their biological properties have been studied, and the most potent compound, **8**, was shown to inhibit TDP1 with an IC_{50} value of 0.16 ± 0.04 μM, to possess low cytotoxicity (CC_{50} value >50 μM), and to enhance the cytotoxicity of the Top1 inhibitor camptothecin by 1 order of magnitude.

RESULTS AND DISCUSSION

Chemistry. Compounds **1**−**11** were synthesized according to Scheme 1. The enamines **1**−**11** were prepared by interaction of (+)- or (−)-usnic acid with the appropriate amines or anilines[33] (Scheme 1).

Scheme 1. Synthesis of Compounds

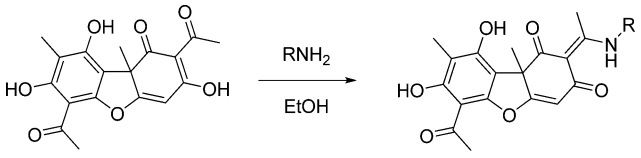

UA 1-11

A 1.1 mmol amount of the appropriate amine was added to 1 mmol of (+)- or (−)-usnic acid, and the mixture was dissolved in 12 mL of ethanol. The reaction mixture was refluxed in a water bath for 3 h and cooled, and then 10 mL of distilled water was added. A light precipitate was formed, which was collected on a filter, washed with water, and dried in air. The precipitate was chromatographed on a silica gel column (fractions 60−200 μM, Merck) by chloroform with a methanol gradient from 0 to 5%.

The structures of the compounds were confirmed by NMR spectroscopy and mass spectrometry.

Biology. We recently designed a new simple fluorophore-quencher-coupled DNA-biosensor for real-time measurement of TDP1 cleavage activity.[32] The substrate is a 16-mer single-stranded oligonucleotide containing both a 5′-FAM fluorophore donor and a quenching 3′-BHQ1 (black hole quencher 1) moiety. The typical curves for BHQ1 removal catalyzed by TDP1 in the presence of the UA enamines are shown in Figure 1.

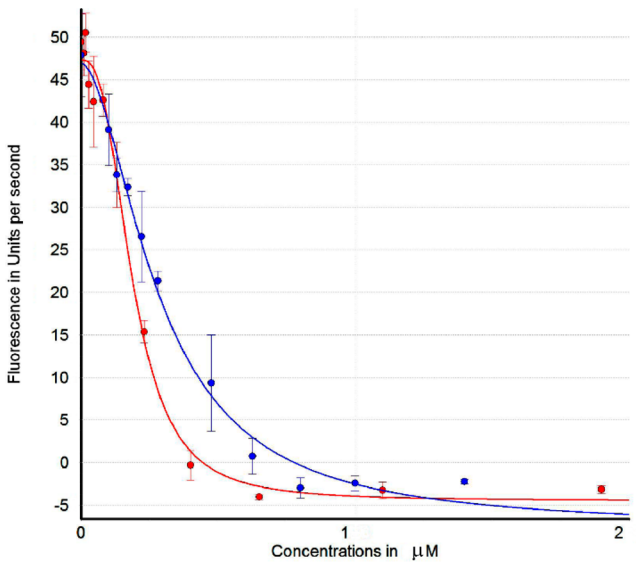

Figure 1. Dependence of TDP1 residual activity as a function of agent concentration. The concentration of TDP1 was 1.3 nM, and TDP1-biosensor concentration was 50 nM. Red graph designates **8**; blue graph designates (+)**5**.

The results for the enamines are presented in Table 1. IC_{50} values ranged from 0.16 to 2.2 μM. The compounds with the best inhibitory properties, **8** and **7**, contained bulky substituent (a 3,5-di-*tert*-butyl-4-hydroxyphenyl ring) and had IC_{50} values of 0.16 and 0.19 μM, respectively. The length of the linker between the UA core and the bulky substituent had no significant effect on the IC_{50} values. Compound **9**, with a hydroxyphenyl ring, was used to elucidate the role of *tert*-butyl groups. The IC_{50} value for this compound was 0.79 μM. The comparison of inhibitors with and without *tert*-butyl groups demonstrated that introduction of this bulky substituent can substantially increase inhibitory activity.

The introduction of a halogen substituent in the phenyl ring increased inhibitory properties and led to IC_{50} values ranging from 0.26 μM (*p*-bromophenyl derivative (+)**5**) to 1.8 μM (*p*-chlorophenyl derivative (+)**4**). The bromophenyl group containing compounds (−)**5**, (+)**5**, and **6** were the most effective inhibitors among halogen derivatives. No substantial influence of angular methyl group orientation was observed (compare enantiomer pairs **1**, **2**, **3**, and **5**). The position of the halogen atom on the phenyl ring also had no effect on IC_{50} values (pairs (−)**2** and **3**; (+)**5** and **6**).

The presence of an aromatic substituent was crucial for enzyme inhibition since compounds **10** (acyclic substituent) and **11** (morpholine substituent) did not inhibit TDP1 in the investigated concentration range.

To validate the data obtained by the fluorescence assay, we performed polyacrylamide gel electrophoretic separation of the Tdp1 reaction products in the presence of compound (+)**5** (Figure 2A). We used the oligonucleotide of the same sequence radiolabeled at the 5′-end, containing the same quencher BHQ1 at the 3′-end. In the absence of the inhibitor, the enzyme removed the BHQ1 residue (lane 1), and the amount

DOI: 10.1021/acs.jnatprod.6b00979
J. Nat. Prod. XXXX, XXX, XXX−XXX

Table 1. Influence of UA Enamines on Activity of Purified TDP1 and MCF-7 Viability in a Single Treatment and in a Combination with Camptothecin

Compound	R	IC_{50}, μM	UA enamines CC_{50}, μM	Camptothecin CC_{50}, nM (in the presence of 0.5 μM UA enamines)	Enhancement of cytotoxicity of camptothecin**
cpt				192±18	
(-)1		1.92 ±0.50	39±20	190±15	1.0
(+)1		1.53±0.71	>50	153±22	1.2
(-)2	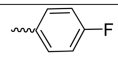	0.94 ±0.42	>50	121±10	1.6
(+)2	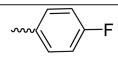	1.54±0.05	22.2	93±51	2.1
3		1.39 ±0.62	35±6	15±5	**12.8**
(-)4	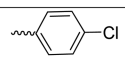	1.62±0.07	16.0±3.1	550±297	0.35
(+)4	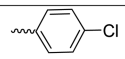	1.81±0.61	>50	375±175	0.51
(-)5	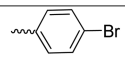	0.57±0.15	10.6±5.2	208±24	0.92
(+)5	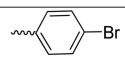	0.26±0.03	39.3±14.9	130±68	1.5
6		0.75±0.33	18.1±3.5	15.3±12.7	**12.5**
7	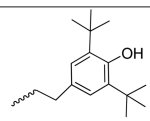	0.19±0.02	>50	115±45	1.7
8	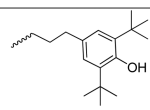	0.16±0.04	>50	18±6	**10.47**
9	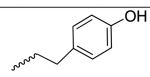	0.79 ±0.19	21.5±2.2	15±3	**12.8**
10	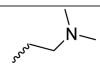	>100	33±13	n/d*	
11	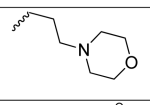	>100	24±1	n/d*	
(+)12	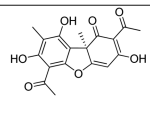	>100	52.3±3.0	n/d*	
(-)12	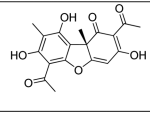	>100	n/d*	n/d*	

*n/d, not determined. **CC_{50} for pure camptothecin/CC_{50} in the presence of the UA enamines ratio. The values for the most effective sensitizers are shown in boldface.

DOI: 10.1021/acs.jnatprod.6b00979
J. Nat. Prod. XXXX, XXX, XXX−XXX

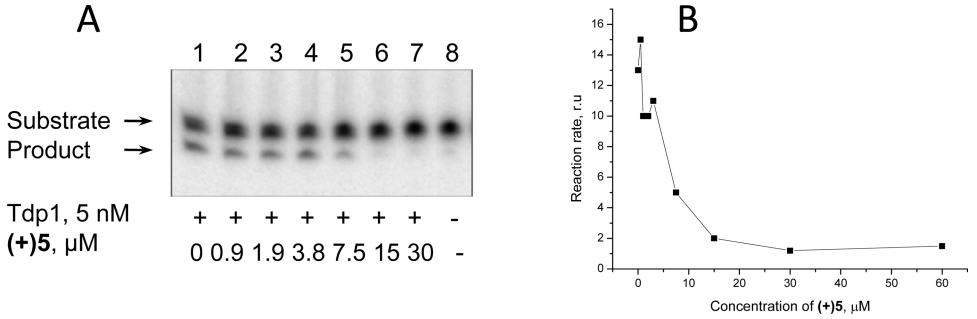

Figure 2. BHQ1 excision from the 3′-end of [^{32}P]-labeled oligonucleotide catalyzed by Tdp1. (A) Electrophoretic separation of the reaction products. Arrows indicate positions of the starting substrate and the reaction product. (B) Typical dependence of the reaction rate on the inhibitor concentration.

of the product decreased with increasing concentration of the inhibitor (lanes 2−8). Figure 2B shows the typical dependence of the reaction rate on the inhibitor concentration. The IC_{50} value for compound (+)**5** was 4.6 μM.

As the usnic acid and its derivatives are known to possess antitumor activity,[4] the UA enamines were tested against the human breast adenocarcinoma cell line MCF-7. The MCF-7 cell line was chosen because of the higher level of Tdp1 gene expression compared to the average according to the BioGPS database (http://biogps.org/#goto=welcome).

The cells were exposed to 0.1 to 100 μM of the compounds. The 50% cytotoxic concentration (CC_{50}) was defined as the concentration required to reduce the cell number by 50% compared to that for the untreated controls. The average CC_{50} values for the compounds shown in Table 1 were derived from three independent experiments. All compounds demonstrated mild cytotoxicity (CC_{50} values were not less than 10 μM). Compound (−)**5** was the most toxic for MCF-7 cells. Compounds (+)**1**, **7**, and **8** demonstrated an unspecific effect on MCF-7 cells: cell survival was reduced compared with the control but was independent of the inhibitor concentration.

Low cytotoxicity of UA enamines (CC_{50} > 10 μM) is crucial for presupposed application in combination with clinically established anticancer drugs. We expect that the use of TDP1 inhibitors would increase the sensitivity of tumor cells to clinical Top1 inhibitors (sensitize tumor cells to the action of Top1 inhibitors). This is expected to reduce the dosage of clinical anticancer drugs and consequently reduce their toxic effects, so the toxicity of TDP1 inhibitors should be minimized.

Camptothecin (CPT) is a natural quinoline alkaloid that inhibits Top1 and possesses anticancer activity.[16] Its bioavailable derivative irinotecan is a key chemotherapeutic drug for metastatic colorectal cancer and other types of tumors.[34] Another CPT derivative, topotecan, is used to treat ovarian cancer when other treatments have failed and to treat certain types of lung cancer (small-cell lung cancer).[35] Since TDP1 removes DNA damage caused by Top1 inhibitors, TDP1 is believed to be responsible for drug resistance of some cancers.[13] For instance, positive correlation between the percentage of non-small-cell lung cancer tumor cells in human tissues and TDP1 activity was observed.[22] Thus, a combination of Top1 and TDP1 inhibitors is expected to improve the efficiency of treatment or allow dose reduction of traditional drugs.

To test this hypothesis, we estimated the cytotoxic effect of CPT in the presence of TDP1 inhibitors. We used a nontoxic concentration of UA enamines (0.5 μM) and different concentrations of CPT to estimate CC_{50} values for MCF-7 cells. The substantial reduction of CC_{50} values in the presence of the TDP1 inhibitors is presented in Figure 3 and Table 1.

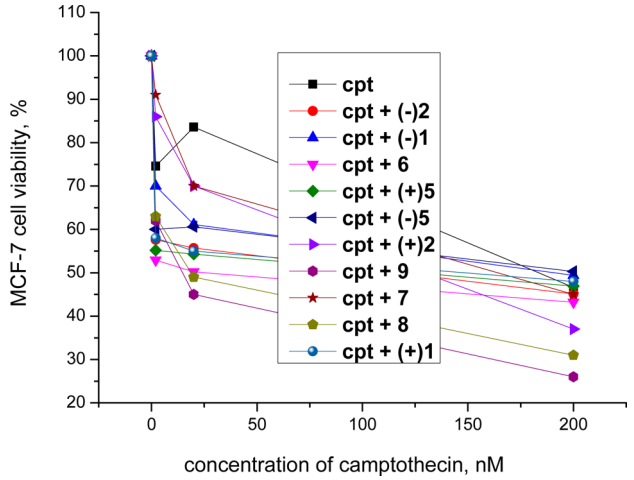

Figure 3. CPT concentration dependence of MCF-7 viability in the presence of UA enamines. MTT assay data.

The presented data show that the most effective sensitizers of MCF-7 cells to CPT (reducing CC_{50} values more than 10 times) were compounds **3**, **6**, **8**, and **9**.

There was no correlation among the level of inhibition of TDP1, toxicity of compounds, and their ability to enhance the effect of CPT (see Table 1). However, one of the promising compounds, **8**, that showed maximum inhibitory activity against TDP1 was nontoxic and enhanced the effect of CPT by 1 order of magnitude.

Since bioavailable derivatives of camptothecin are used for the treatment a lung cancer, we examined the effect of UA enamines against A-549 cells (adenocarcinomic human alveolar basal epithelial cells). Four of the most effective sensitizers of MCF-7 cells to CPT were chosen: **3**, **6**, **8**, and **9**. Cytotoxicity of these compounds against A-549 cells and their influence on CPT cytotoxic effect are shown in Table 2.

The UA enamines also sensitized A-549 cells to camptothecin, though not as efficiently as MCF-7 cells. Compound **8** enhanced CPT cytotoxic effects 3.5 times (Figure 4). Most likely, this difference can be explained by different levels of Tdp1 gene expression in these cell lines. The level of protein expression in MCF-7 cells is 10-fold higher than that in A-549 cells according to the data of Proteomics DB (https://www.proteomicsdb.org). In addition, the ratio of protein to mRNA of MCF-7 cells is significantly higher than in A-549 cells.

DOI: 10.1021/acs.jnatprod.6b00979
J. Nat. Prod. XXXX, XXX, XXX−XXX

Table 2. Influence of UA Enamines on A-549 Viability as a Monopreparation or in Combination with Camptothecin

Compound	R	UA enamines CC_{50}, μM	Camptothecin CC_{50}, nM (in the presence of 0.5 μM UA enamines)	Enhancement of cytotoxicity of camptothecin*
cpt			156±33	
3		>100	96±9	**1.6**
6		>100	135±12	**1.2**
8	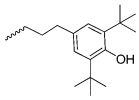	>100	44±5	**3.5**
9	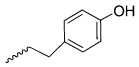	70	124±10	**1.3**

*CC_{50} for pure camptothecin/CC_{50} in the presence of the UA enamines ratio. The values for the most effective sensitizers are shown in boldface.

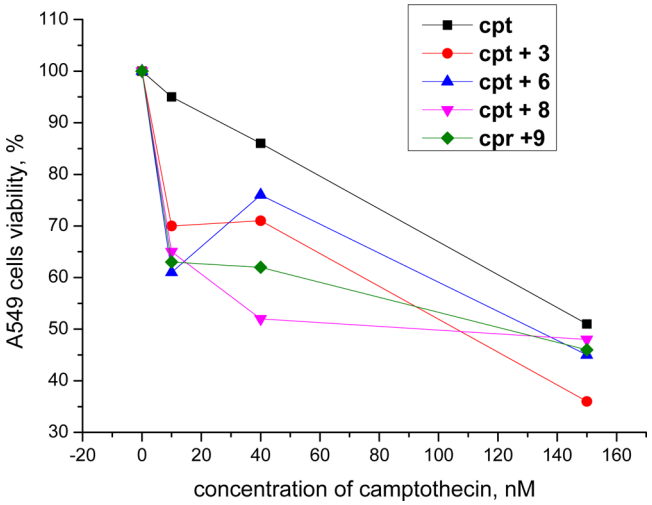

Figure 4. CPT concentration dependence of A-549 viability in the presence of UA enamines. MTT assay data.

Molecular Modeling. In the proposed two-step catalytic mechanism of TDP1, conserved residues His263 and His493 act as a nucleophile and general acid/base, respectively.[36−38] In the first step of the reaction, His263 attacks the 3′-phosphotyrosyl bond of the substrate. The covalent 3′-phosphohistidine intermediate is formed, and the leaving group is protonated by His493. In the second step, the water molecule activated by His493 acts as a nucleophile, and the 3′-phosphohistidine intermediate is hydrolyzed to produce 3′-phosphate DNA. TDP1's catalytic cycle offers two potential therapeutic strategies: (1) the inhibition of the first step to prevent the phosphoryl transfer and (2) the inhibition of the second step to prevent the hydrolysis of the DNA−protein intermediate.[11] The second approach could somehow be similar to the stabilization of Top1−DNA covalent complexes by camptothecins.[15,39]

We have modeled three forms of TDP1 enzyme that represent targets for potential inhibitors: the apo form, the enzyme−substrate complex, and the covalent phosphohistidine intermediate (Figure 5A−C). Models A and B were designed to

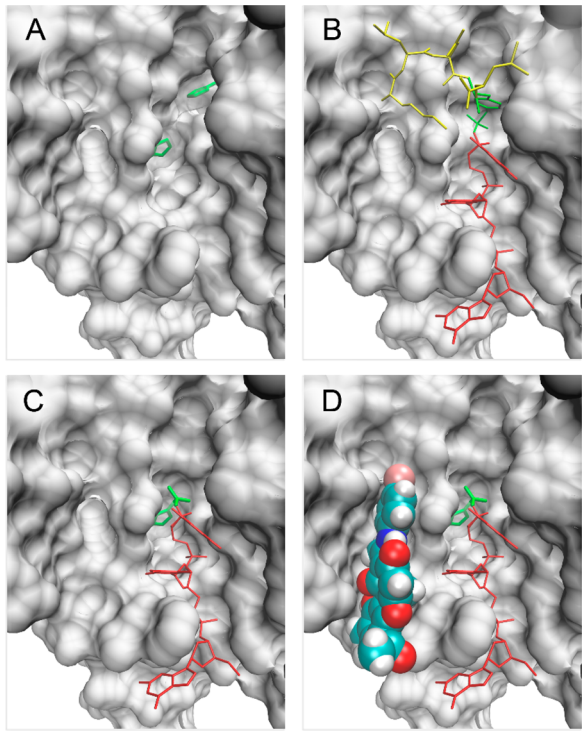

Figure 5. Molecular models of the TDP1 structure. (A) The apo form. Catalytic residues His263 and His493 are shown in green. (B) The enzyme−substrate complex. The oligonucleotide is shown in red, 3′-phosphotyrosine is shown in green, and the rest of the peptide is shown in yellow. (C) The covalent intermediate. 3′-Phosphohistidine is shown in green. (D) The ternary complex with an inhibitor, (+)**5**. The inhibitor molecule is colored by atom type.

simulate interaction with inhibitors of the first step of the reaction, while model C represents a target for intermediate-stabilizing inhibitors of the second step. Enamines of usnic acid were found to bind preferentially to the phosphohistidine intermediate occupying a cavity adjacent to the active site of TDP1 (Figure 5D). This cavity is formed by residues Tyr204, Cys205, Asp230, Lys231, Leu255 Ala258, Phe259, and Thr261, which are able to mediate hydrophobic and hydrogen-bonding interactions with a low-molecular-weight ligand. We hypothesize that enamine inhibitors in a ternary complex with TDP1 affect the conformation of the Tyr204, Cys205, Phe259, and Thr261 residues located at the boundary between the active site and the inhibitor's cavity, thus disrupting the reactive orientation of the phosphohistidine intermediate and nucleophilic water molecule.

Conclusions. Our research has revealed a new class of UA enamine derivatives as TDP1 inhibitors. Compounds **7** and **8**, containing 3,5-di-*tert*-butyl-4-hydroxyphenyl substituents, demonstrated inhibitory activity in the high nanomolar concentration range and to our knowledge were the most potent TDP1 suppressors.

All compounds possessed low toxicity against human MCF-7 and A-549 tumor cells, and some of the UA enamines were able to enhance the cytotoxicity of camptothecin. The most promising compound, **8**, had maximum inhibitory activity against TDP1, was nontoxic in the investigated concentration

DOI: 10.1021/acs.jnatprod.6b00979
J. Nat. Prod. XXXX, XXX, XXX−XXX

range, and was able to improve the cytotoxic effect of camptothecin by 10-fold.

According to the modeling results, UA enamines bind preferentially to the covalent DNA−protein intermediate at the second step of the reaction.

EXPERIMENTAL SECTION

Chemistry. The analytical and spectral studies were conducted in the Chemical Service Center for the collective use of SB RAS.

The ^{1}H and ^{13}C NMR spectra for solutions of the compounds in $CDCl_3$ were recorded on a Bruker AV-400 spectrometer (400.13 and 100.61 MHz, respectively). The residual signals of the solvent were used as references (δ_H 2.48, δ_C 39.52). The mass spectra (70 eV) were recorded on a DFS Thermo Scientific high-resolution mass spectrometer. The melting points were measured using a Kofler heating stage. The specific rotation was determined on a PolAAr 3005 and is provided in (deg × mL) × (g × dm)$^{-1}$, where the concentration of the solutions is shown in g × (100 × mL)$^{-1}$. Merck silica gel (63−200 μm) was used for the column chromatography. Thin-layer chromatography was performed on Silufol plates (UV-254).

The atom numbering in the compounds was provided for the assignment of signals in the NMR spectra and is different from the atom numbering in the nomenclature name. The target compounds reported here have a purity of at least 97% (HPLC).

Compounds **10** and **11** were synthesized as described by Luzina et al.[40] Compounds (+)**1**, (−)**1**, (+)**4**, (−)**4**, (+)**5**, and (−)**5** were synthesized as described previously.[41] Compounds **7** and **8** were synthesized as described by Tazetdinova et al.[33] Compounds (+)**2**, (−)**2**, **3**, and **6** were synthesized as described by Sokolov et al.[42]

Compound 9. Compound (+)**12** (1 mmol) was treated with 4-hydroxyphenethylamine (1.1 mmol). The mixture was dissolved in EtOH (12 mL), refluxed on a water bath for 3 h, cooled, and treated with distilled H_2O (10 mL). The light precipitate was filtered off, rinsed with H_2O, and dried in air. Compound **9** was isolated by column chromatography over silica gel with elution by a gradient of MeOH in CH_2Cl_2 (from 0 to 10%).

(*R*,*E*)-6-Acetyl-7,9-dihydroxy-2-(1-(4-hydroxyphenethylamino)ethylidene)-8,9b-dimethyldibenzo-[*b*,*d*]furan-1,3(2*H*,9b*H*)-dione, 9: yellow, amorphous powder. Yield: 78%; mp 116 °C; $[\alpha]^{28}_D$ +254 (*c* 0.22, $CHCl_3$); ^{1}H NMR ($CDCl_3$, δ, *J* Hz) 1.70 (3H, s, H-15), 2.11 (3H, s, H-10), 2.57 (3H, s, H-12), 2.67 (3H, s, H-14), 2.96 (2H, t, *J* = 6.7, H-17), 3.73 (2H, dt, *J* = 6.7 and 5.5, H-16), 5.81 (1H, s, H-4), 6.81 (2H, d, *J* = 8.3, H-3′ and H-5′), 7.11 (2H, d, *J* = 8.3, H-2′ and H-6′), 11.89 (1H, s, OH-9), 13.22 (1H, bs, NH), 13.59 (1H, s, OH-7); ^{13}C NMR ($CDCl_3$, δ) 7.27 (C-10), 18.15 (C-12), 31.04 (C-14), 31.76 (C-15), 34.11 (C-17), 45.54 (C-16), 57.01 (C-9b), 101.15 (C-6), 102.03 (C-4), 102.60 (C-2), 104.81 (C-9a), 107.84 (C-8), 115.70 (C-3′ and C-5′), 129.68 (C-1′), 129.68 (C-2′ and C-6′), 155.11 (C-4′), 155.64 (C-5a), 158.00 (C-9), 163.25 (C-7), 174.80 (C-11), 174.7 (C-4a), 189.9 (C-3), 198.14 (C-1), 200.53 (C-13); MS *m*/*z* found 463.1620 $[M]^+$ $C_{26}H_{25}O_7N$, calcd M = 463.1626.

Biology. The recombinant TDP1 was purified to homogeneity by chromatography on Ni-chelating resin and phosphocellulose P11 as described[43,44] using plasmid pET 16B-Tdp1 kindly provided by Dr. K. W. Caldecott (University of Sussex, United Kingdom).

TDP1-biosensor 5′-(5,6 FAM-aac gtc agg gtc ttc c-BHQ1)-3′ was synthesized in the Laboratory of Medicinal Chemistry, Institute of Chemical Biology and Fundamental Medicine, Novosibirsk, Russia.

Real-Time Detection of TDP1 Activity. The TDP1 activity measurements were carried out as described.[32] Briefly, TDP1-biosensor with a final concentration of 50 nM was incubated in a volume of 200 μL containing TDP1 buffer (50 mM Tris-HCl pH8,0, 50 mM NaCl, 7 mM β-mercaptoethanol) supplemented with purified 1.3 nM TDP1. The reactions were incubated at a constant temperature of 26 °C in a POLARstar OPTIMA fluorimeter, BMG LABTECH, GmbH, to measure fluorescence every 1 min (Ex_{485}/Em_{520} nm). TDP1 inhibition was calculated by comparing the rate of increase in fluorescence in the presence of compound to that of DMSO control wells. IC_{50} values were determined using an 11-point concentration response curve. The data were imported into the MARS Data Analysis 2.0 program (BMG LABTECH), and the slope during the linear phase (here data from 0 to 7 min) was calculated.

Gel-Based Enzyme Assay. The [^{32}P]-label at the 5′-end of the oligonucleotide was carried out using T4 polynucleotide kinase, and the labeled oligonucleotide was purified by electrophoresis in a denaturing polyacrylamide gel in the presence of 7 M urea. The reaction mixture contained 50 nM DNA substrate, 5 nM Tdp1, 50 mM Tris-HCl, 50 mM NaCl, 7 mM β-mercaptoethanol, and the inhibitor (+)**5** in a concentration 0−60 μM. The reaction was conducted at 26 °C for 20 min. The reaction products were separated by electrophoresis on 20% denaturing polyacrylamide gel with 7 M urea. A Typhoon FLA 9500 phosphorimager (GE Healthcare) was used for gel scanning and imaging, and the data were analyzed with QuantityOne 4.6.7 software. IC_{50} values were determined using OriginPro 8.6.0 software.

Cell Culture Assays. Tumor cells from human mammary adenocarcinoma cell lines MCF-7 (~2000 cells per well) were incubated for 24 h at 37 °C in IMDM medium (5% CO_2), and then they were treated with the UA enamines. After 72 h of cell incubation the relative amount of alive cells was determined using 3-[4,5-dimethylthiazol-2-yl]-2,5-diphenyl tetrazolium bromide (standard colorimetric MTT test),[45] and the drug concentration that causes 50% cell growth inhibition (CC_{50}) was determined.

Molecular Modeling. Three TDP1 models were used in docking studies: (A) "apo form", (B) "enzyme−substrate complex", and (C) "covalent intermediate". Model B was built on the basis of the 1nop crystal structure with a substrate analogue[46] and energy minimized using a QM/MM implementation in Amber 12.[47] The 3′-terminal nucleotide with a covalently attached tyrosyl moiety and the side chains of His263 (with protonated $N^{\delta1}$-atom) and His493 (with protonated both $N^{\delta1}$ and $N^{\varepsilon2}$ atoms) were treated quantum mechanically at the RM1 level of theory.[48] Model A was obtained by removing the substrate molecule from model B. Model C was constructed by applying a harmonic restraint on the distance between 3′-phosphate and His263 in model B to drive the covalent bond formation. The PO_4:P···His263:$N^{\varepsilon2}$ distance was reduced by the restrained QM/MM minimization, and then the unrestrained energy minimization was carried out to obtain the relaxed intermediate structure. Finally, the tyrosyl-containing peptide, the first reaction product, was removed from the active site.

The structures of TDP1 inhibitors were optimized by ACD/ChemSketch.[49] Molecular docking of compounds into models A−C was performed with the Lead Finder 1.1.16 software.[50] In docking experiments, an energy grid box with edges of 35 Å was centered on the $N^{\varepsilon2}$ atom of His493. VMD 1.9.2[51] was used to visualize the obtained models of TDP1-inhibitor complexes.

ASSOCIATED CONTENT

Supporting Information

The Supporting Information is available free of charge on the ACS Publications website at DOI: 10.1021/acs.jnatprod.6b00979.

NMR ^{1}H, ^{13}C, and mass spectra of compound **9** (PDF)

AUTHOR INFORMATION

Corresponding Author

*E-mail: lavrik@niboch.nsc.ru. Tel: +7(383)3635196.

Author Contributions

#A. Zakharenko and O. Luzina contributed equally to this research.

Notes

The authors declare no competing financial interest.

DOI: 10.1021/acs.jnatprod.6b00979
J. Nat. Prod. XXXX, XXX, XXX−XXX

■ ACKNOWLEDGMENTS

This work was supported by the Ministry of Education and Science of Russian Federation, State Agreement RFME-FI60414X0018.

■ REFERENCES

(1) Ingolfsdottir, K. *Phytochemistry* **2002**, *61*, 729−736.
(2) Guo, L.; Shi, Q.; Fang, J. L.; Mei, N.; Ali, A. A.; Lewis, S. M.; Leakey, J. E.; Frankos, V. H. *J. Environ. Sci. Health* **2008**, *26*, 317−338.
(3) Luzina, O. A.; Salakhutdinov, N. F. *Russ. J. Bioorg. Chem.* **2016**, *42*, 115−132.
(4) Luzina, O. A.; Salakhutdinov, N. F. *Russ. J. Bioorg. Chem.* **2016**, *42*, 249−268.
(5) Sokolov, D. N.; Luzina, O. A.; Salakhutdinov, N. F. *Russ. Chem. Rev.* **2012**, *8*, 747−768.
(6) Yu, X.; Guo, Q.; Su, G.; Yang, A.; Hu, Zh.; Qu; Ch; Wan; Li, R.; Tu, P.; Chai, X. *J. Nat. Prod.* **2016**, *79*, 1373−1380.
(7) Bazin, M. A.; Le Lamer, A. C.; Delcros, J. G.; Rouaud, I.; Uriac, P.; Boustie, J.; Corbel, J. C.; Tomasi, S. *Bioorg. Med. Chem.* **2008**, *16*, 6860−6866.
(8) Sykora, P.; Wilson, D. M., III; Bohr, V. A. *Mech. Ageing Dev.* **2013**, *134*, 440−448.
(9) Virag, L.; Szabo, C. *Pharmacol Rev.* **2002**, *54*, 375−429.
(10) Shukla, P. C.; Singh, K. K.; Yanagawa, B.; Teoh, H.; Verma, S. *Can. J. Cardiol.* **2010**, *26*, 13A.
(11) Comeaux, E. Q.; van Waardenburg, R. C. *Drug Metab. Rev.* **2014**, *46*, 494−507.
(12) Alagoz, M.; Wells, O. S.; El-Khamisy, S. F. *Nucleic Acids Res.* **2014**, *42*, 3089.
(13) Dexheimer, T. S.; Antony, S.; Marchand, C.; Pommier, Y. *Anti-Cancer Agents Med. Chem.* **2008**, *8*, 381−389.
(14) Yang, S. W.; Burgin, A. B., Jr.; Huizenga, B. N.; Robertson, C. A.; Yao, K. C.; Nash, H. A. *Proc. Natl. Acad. Sci. U. S. A.* **1996**, *93*, 11534−11539.
(15) Pommier, Y.; Leo, E.; Zhang, H.; Marchand, C. *Chem. Biol.* **2010**, *17*, 421−433.
(16) Pommier, Y. *Nat. Rev. Cancer* **2006**, *6*, 789−802.
(17) Beretta, G. L.; Cossa, G.; Gatti, L.; Zunino, F.; Perego, P. *Curr. Med. Chem.* **2010**, *17*, 1500−1508.
(18) El-Khamisy, S. F.; Katyal, S.; Patel, P.; Ju, L.; McKinnon, P. J.; Caldecott, K. W. *DNA Repair* **2009**, *8*, 760−766.
(19) Das, B. B.; Antony, S.; Gupta, S.; Dexheimer, T. S.; Redon, C. E.; Garfield, S.; Shiloh, Y.; Pommier, Y. *EMBO J.* **2009**, *28*, 3667−3680.
(20) Katyal, S.; el-Khamisy, S. F.; Russell, H. R.; Li, Y.; Ju, L.; Caldecott, K. W.; McKinnon, P. J. *EMBO J.* **2007**, *26*, 4720−4731.
(21) Hirano, R.; Interthal, H.; Huang, C.; Nakamura, T.; Deguchi, K.; Choi, K.; Bhattacharjee, M. B.; Arimura, K.; Umehara, F.; Izumo, S.; Northrop, J. L.; Salih, M. A.; Inoue, K.; Armstrong, D. L.; Champoux, J. J.; Takashima, H.; Boerkoel, C. F. *EMBO J.* **2007**, *26*, 4732−4743.
(22) Jakobsen, A. K.; Lauridsen, K. L.; Samuel, E. B.; Proszek, J.; Knudsen, B. R.; Hager, H.; Stougaard, M. *Exp. Mol. Pathol.* **2015**, *99*, 56−64.
(23) Cortes Ledesma, F.; El Khamisy, S. F.; Zuma, M. C.; Osborn, K.; Caldecott, K. W. *Nature* **2009**, *461*, 674−678.
(24) Antony, S.; Marchand, C.; Stephen, A. G.; Thibaut, L.; Agama, K. K.; Fisher, R. J.; Pommier, Y. *Nucleic Acids Res.* **2007**, *35*, 4474−4484.
(25) Nguyen, T. X.; Morrell, A.; Conda-Sheridan, M.; Marchand, C.; Agama, K.; Bermingam, A.; Stephen, A. G.; Chergui, A.; Naumova, A.; Fisher, R.; O'Keefe, B. R.; Pommier, Y.; Cushman, M. *J. Med. Chem.* **2012**, *55*, 4457−4478.
(26) Conda-Sheridan, M.; Reddy, P. V. N.; Morrell, A.; Cobb, B. T.; Marchand, C.; Agama, K.; Chergui, A.; Renaud, A.; Stephen, A. G.; Bindu, L. K.; Pommier, Y.; Cushman, M. *J. Med. Chem.* **2013**, *56*, 182−200.
(27) Sirivolu, V. R.; Vernekar, S. K.; Marchand, C.; Naumova, A.; Chergui, A.; Renaud, A.; Stephen, A. G.; Chen, F.; Sham, Y. Y.; Pommier, Y.; Wang, Z. *J. Med. Chem.* **2012**, *55*, 8671−8684.
(28) Huang, S. N.; Pommier, Y.; Marchand, C. *Expert Opin. Ther. Pat.* **2011**, *21*, 1285−1292.
(29) Davies, D. R.; Interthal, H.; Champoux, J. J.; Hol, W. G. J. *J. Mol. Biol.* **2003**, *324*, 917−932.
(30) Marchand, C.; Lea, W. A.; Jadhav, A.; Dexheimer, T. S.; Austin, C. P.; Inglese, J.; Pommier, Y.; Simeonov, A. *Mol. Cancer Ther.* **2009**, *8*, 240−248.
(31) Zakharenko, A. L.; Ponomarev, K.; Yu; Suslov, E. V.; Korchagina, D. V.; Volcho, K. P.; Vasil'eva, I. A.; Salakhutdinov, N. F.; Lavrik, O. I. *Russ. J. Bioorg. Chem.* **2015**, *41*, 657−662.
(32) Zakharenko, A. L.; Khomenko, T. M.; Zhukova, S. V.; Koval, O. A.; Zakharova, O. D.; Anarbaev, R. O.; Lebedeva, N. A.; Korchagina, D. V.; Komarova, N. I.; Vasiliev, V. G.; Reynisson, J.; Volcho, K. P.; Salakhutdinov, N. F.; Lavrik, O. I. *Bioorg. Med. Chem.* **2015**, *23*, 2044−2052.
(33) Tazetdinova, A. A.; Luzina, O. A.; Polovinka, M. P.; Salakhutdinov, N. F.; Tolstikov, G. A. *Chem. Nat. Compd.* **2009**, *45*, 800.
(34) Dancey, J.; Eisenhauer, E. A. *Br. J. Cancer* **1996**, *74*, 327−338.
(35) Fujita, K.; Kubota, Y.; Ishida, H.; Sasaki, Y. *World J. Gastroenterol.* **2015**, *21*, 12234−12248.
(36) Davies, D. R.; Interthal, H.; Champoux, J. J.; Hol, W. G. J. *Structure* **2002**, *10*, 237−248.
(37) Gajewski, S.; Comeaux, E. Q.; Jafari, N.; Bharatham, N.; Bashford, D.; White, S. W.; van Waardenburg, R. C. *J. Mol. Biol.* **2012**, *415*, 741−758.
(38) DeYonker, N. J.; Webster, C. E. *Biochemistry* **2015**, *54*, 4236−4247.
(39) Staker, B. L.; Hjerrild, K.; Feese, M. D.; Behnke, C. A.; Burgin, A. B., Jr.; Stewart, L. *Proc. Natl. Acad. Sci. U. S. A.* **2002**, *99*, 15387−15392.
(40) Luzina, O. A.; Sokolov, D. N.; Pokrovskii, M. A.; Pokrovskii, A. G.; Bekker, O. B.; Danilenko, V. N.; Salakhutdinov, N. F. *Chem. Nat. Compd.* **2015**, *51*, 646−651.
(41) Zakharenko, A.; Sokolov, D.; Luzina, O.; Sukhanova, M.; Khodyreva, S.; Zakharova, O.; Salakhutdinov, N.; Lavrik, O. *Med. Chem.* **2012**, *8*, 883−893.
(42) Sokolov, D. N.; Zarubaev, V. V.; Shtro, A. A.; Polovinka, M. P.; Luzina, O. A.; Komarova, N. I.; Salakhutdinov, N. F.; Kiselev, O. I. *Bioorg. Med. Chem. Lett.* **2012**, *22*, 7060−7064.
(43) Interthal, H.; Pouliott, J. J.; Champoux, J. J. *Proc. Natl. Acad. Sci. U. S. A.* **2001**, *98*, 12009−12014.
(44) Lebedeva, N. A.; Rechkunova, N. I.; Lavrik, O. I. *FEBS Lett.* **2011**, *585*, 683−686.
(45) Mosmann, T. *J. Immunol. Methods* **1983**, *65*, 55−63.
(46) Davies, D. R.; Interthal, H.; Champoux, J. J.; Hol, W. G. J. *Chem. Biol.* **2003**, *10*, 139−147.
(47) Case, D. A.; Darden, T. A.; Cheatham, T. E., 3rd; Simmerling, C. L.; Wang, J.; Duke, R. E.; Luo, R.; Walker, R. C.; Zhang, W.; Merz, K. M.; Roberts, B.; Hayik, S.; Roitberg, A.; Seabra, G.; Swails, J.; Götz, A. W.; Kolossváry, I.; Wong, K. F.; Paesani, F.; Vanicek, J.; Wolf, R. M.; Liu, J.; Wu, X.; Brozell, S. R.; Steinbrecher, T.; Gohlke, H.; Cai, Q.; Ye, X.; Wang, J.; Hsieh, M.-J.; Cui, G.; Roe, D. R.; Mathews, D. H.; Seetin, M. G.; Salomon-Ferrer, R.; Sagui, C.; Babin, V.; Luchko, T.; Gusarov, S.; Kovalenko, A.; Kollman, P. A. *AMBER 12*; University of California: San Francisco, 2012.
(48) Rocha, G. B.; Freire, R. O.; Simas, A. M.; Stewart, J. J. P. *J. Comput. Chem.* **2006**, *27*, 1101−1111.
(49) *ACD/ChemSketch* (Freeware) 2015; Advanced Chemistry Development, Inc., http://www.acdlabs.com.
(50) Stroganov, O. V.; Novikov, F. N.; Stroylov, V. S.; Kulkov, V.; Chilov, G. G. *J. Chem. Inf. Model.* **2008**, *48*, 2371−2385.
(51) Humphrey, W.; Dalke, A.; Schulten, K. *J. Mol. Graphics* **1996**, *14*, 33−38.

DOI: 10.1021/acs.jnatprod.6b00979
J. Nat. Prod. XXXX, XXX, XXX−XXX